universe

MDPI

Communication

Searches for Electric Dipole Moments—Overview of Status and New Experimental Efforts †

Florian Kuchler on behalf of the TUCAN and HeXeEDM Collaborations

Physical Sciences Division, TRIUMF, Vancouver, BC V6T 2A3, Canada; fkuchler@triumf.ca

† This paper is based on the talk at the 7th International Conference on New Frontiers in Physics (ICNFP 2018), Crete, Greece, 4–12 July 2018.

Received: 31 December 2018; Accepted: 3 February 2019; Published: 9 February 2019

Abstract: Searches for permanent electric dipole moments (EDMs) of fundamental particles, atoms and molecules are promising experiments to constrain and potentially reveal beyond Standard Model (SM) physics. A non-zero EDM is a direct manifestation of time-reversal (T) violation, and, equivalently, violation of the combined operation of charge-conjugation (C) and parity inversion (P). Identifying new sources of CP violation can help to solve fundamental puzzles of the SM, e.g., the observed baryon-asymmetry in the Universe. Theoretical predictions for magnitudes of EDMs in the SM are many orders of magnitude below current experimental limits. However, many theories beyond the SM require larger EDMs. Experimental results, especially when combined in a global analysis, impose strong constraints on CP violating model parameters. Including an overview of EDM searches, I will focus on the future neutron EDM experiment at TRIUMF (Vancouver). For this effort, the TUCAN (TRIUMF Ultra Cold Advanced Neutron source) collaboration is aiming to build a strong, world leading source of ultra cold neutrons (UCN) based on a unique combination of a spallation target and a superfluid helium UCN converter. Another focus will be the search for an EDM of the diamagnetic atom ^{129}Xe using a ^{3}He comagnetometer and SQUID detection. The HeXeEDM collaboration has taken EDM data in 2017 and 2018 in the magnetically shielded room (BMSR-2) at PTB Berlin.

Keywords: electric dipole moment; EDM; CP violation; new physics; neutron; xenon

1. Introduction

The Standard Model (SM) of particle physics describes many experimental observations with impressive accuracy and successfully withstands many experimental tests. However, there are yet unsolved puzzles that require an extended theory beyond the SM. Among others, three main issues to be addressed are dark energy, the nature of dark matter and the observed baryon asymmetry in our Universe. The latter is apparent from observations of the cosmic microwave background (CMB) [1] and big bang nucleosynthesis (BBN) [2], from which the ratio of the difference in matter and anti-matter number density to the number density of photons n_γ in our Universe can be determined to be

$$\frac{n_\mathrm{B} - n_{\bar{\mathrm{B}}}}{n_\gamma} \approx 10^{-10}, \tag{1}$$

with n_B and $n_{\bar{\mathrm{B}}}$ being the number densities of barionic matter and anti-matter, respectively. In contrast, the SM expectation for this ratio is about eight orders of magnitude smaller. According to Sakharov [3], there are three conditions to be fulfilled for the Universe to evolve into a state of baryon asymmetry: (i) departure from thermal equilibrium; (ii) baryon number violation and (iii) C and CP violation. These conditions can in principal be accounted for within the SM, i.e., through so-called "sphaleron" processes and electroweak symmetry breaking [4]. The last condition (iii) involves breaking of fundamental

symmetries by charge-conjugation (C) and the subsequent operation of parity- and charge-conjugation (CP). The SM provides CP violation via a complex phase in the CKM matrix and through the θ term in strong interactions, but the known mechanisms can not account for the observed baryon asymmetry. Hence, a more complete theory requires additional CP violation and experimental programs searching for its signatures are of great interest to identify the underlying physics.

Searches for electric dipole moments (EDMs) of fundamental particles, molecules and atoms offer a sensitive, direct probe of these underlying new physics. A non-zero EDM violates both parity (P) and time-reversal (T) symmetries (Figure 1). Hence, assuming CPT to be a good symmetry, a non-zero EDM is also a manifestation of CP violation and obtained experimental limits can put strong constraints on theories beyond the SM that usually require more CP violation.

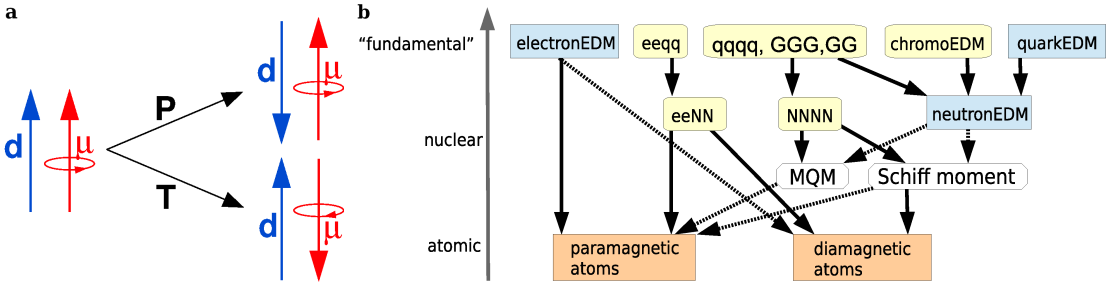

Figure 1. (**a**) a non-zero electric dipole moment (EDM) d aligned with the magnetic moment μ violates both parity (P) and time-reversal (T) symmetry. Hence, assuming CPT—with C refering to charge-conjugation—to be conserved, $d \neq 0$ also violates CP symmetry; (**b**) CP violating sources contributing to EDMs in various systems on different energy scales. Fundamental particle EDMs (blue boxes) as wells as CP-odd interactions (yellow boxes) between electrons (e), quarks (q) and gluons (G) lead to EDMs of complex systems like atoms (orange boxes). Nuclear moments (white boxes) of atoms, e.g., magnetic quadrupole moments (MQM) and Schiff moments [5], arise from CP-odd sources.

2. EDM Experiments Overview

In the SM, EDMs arise from two mechanisms. In QCD, the θ term ($\sim \bar{\theta} G\tilde{G}$) is the leading CP-odd contribution in the Lagrangian [6]. However, experimental results of the neutron EDM [7] put strong constraints on $\bar{\theta}$ via $d_\mathrm{n} \sim \bar{\theta} \cdot (6 \times 10^{-17})$ $e$cm, leading to an unnaturally small $\bar{\theta} < 10^{-10}$ [6]. A possible solution to this "Strong CP-problem" was initially proposed by introducing a new particle, the axion [8], resulting in a now very active field of axion searches. Generation of CP violation in the weak interaction through the CKM matrix is only a higher order effect, e.g., with the largest contribution to an EDM of the neutron being $d_\mathrm{n}^\mathrm{CKM} \sim 10^{-32}$ $e$cm [9]. Predictions of EDMs in the SM are small (c.f. Table 1) compared to theories beyond the SM, which generally introduce more CP violation and require larger EDMs. Hence, upper limits from EDM searches can help constrain the model parameters of beyond SM theories.

A summary of the most recent published upper limits for EDMs of various systems of interest and their SM predictions are shown in Table 1. As EDMs in fundamental particles and atoms arise from different sources of underlying CP-odd physics, a combination of experimental results in a global analysis is beneficiary over a sole-source analysis. The diagram in Figure 1 shows an overview of major (solid lines) and minor (dashed lines) CP violating contributions to EDMs of fundamental particles and atoms on various energy scales. The EDM of the neutron has contributions from quark EDMs and chromo EDMs as well as CP-odd interactions of quarks and gluons. However, atomic EDMs arise from intrinsic EDMs of unpaired electrons or nucleons and CP-odd interactions of both nucleons and electrons. For diamagnetic atoms, like ^{129}Xe, an EDM of the nucleus is screened by the closed electron shell. However, imperfect screening of the nuclear EDM due to finite size effects leads to an observable atomic moment, the so-called Schiff moment [5].

Table 1. Summary of published experimental upper limits and Standard Model (SM) predictions for several systems of fundamental particles and atoms used in electric dipole moment (EDM) searches. Experimental results are far beyond SM predictions but are within reach of beyond SM theories to constrain model parameters.

	Neutron	**Electron**	**^{199}Hg**	**^{129}Xe**	**^{225}Ra**	**Ref.**
	95% C.L.	**90% C.L.**	**95% C.L.**	**95% C.L.**	**95% C.L.**	
Exp. upper limit ($e$cm)	3.6×10^{-26}	1.1×10^{-29}	7.4×10^{-30}	6.6×10^{-27}	1.4×10^{-24}	[7,10–13]
SM pred. ($e$cm)	$\sim 10^{-31} - 10^{-32}$	$\sim 10^{-38}$	$\sim 10^{-34}$	$\sim 10^{-34}$	-	[14–17]

In a global analysis, the results of different systems can be combined to improve upper bounds on individual CP-odd contributions [18]. As an example, an improved limit on the EDM of ^{129}Xe by one to two orders of magnitude can significantly improve constraints on particular electron–nucleon (C_T) and nucleon–nucleon ($\bar{g}_\pi^{(0)}$) interactions, although the result would still be far from the superior upper limit on the EDM of ^{199}Hg. The prospect of these improvements and possible use as an additional comagnetometer in future neutron EDM experiments [19] encourages experimental efforts with better sensitivity on the EDM of ^{129}Xe. Heavy elements with deformed nuclei like ^{225}Ra are promising candidates due to strong nuclear enhancement effects [12]. First results have recently been published with expected significant improvements in the near future.

The general technique to search for an EDM d is to place a spin polarized species (e.g., spin 1/2) in an applied magnetic and electric field and determine the difference in Larmor precession frequencies $\Delta\omega$ for magnetic and electric fields aligned in parallel and anti-parallel:

$$d = \frac{\hbar \Delta\omega}{4E}, \tag{2}$$

assuming the magnetic field is equal for both measurements and $|E^{\uparrow}| = |E^{\downarrow}| = E$. The rather simple method comes with technical challenges, e.g., correction of magnetic field drifts, in particular when they are correlated with electric field reversal. It is interesting to note that an EDM sensitivity of $\sigma_\mathrm{d} \sim 10^{-27}$ $e$cm typically (assuming $E \sim 10$ kV/cm) corresponds to a frequency sensitivity of $\sigma_\mathrm{f} \sim 10^{-9}$ Hz and—for nuclear magnetic moments—to a magnetic field variation of only $\delta B \sim 10^{-16}$ T. An overview of the history of experimental progress in EDM results for neutrons, atoms and the electron is shown in Figure 2. In the remainder, the focus will be on experiments searching for an EDM of the neutron, particularly the neutron EDM project at TRIUMF and recent efforts of the HeXeEDM collaboration to improve sensitivity for the EDM of the diamagnetic atom ^{129}Xe.

3. Neutron EDM Experimental Status

The neutron is a simple system in terms of the fundamental contributions to it's EDM (c.f. Figure 1). First measurements in the 1950s were based on neutron beams superseded in the 1980s by storage experiments using ultra cold neutrons (UCN) (see Figure 2).

Most next generation neutron EDM searches are using UCN with energies below a few hundreds of neV. UCN can be stored for long periods of several hundreds of seconds using wall materials with a high Fermi potential. Suitable choices are e.g., copper (∼170 neV), stainless steel (∼190 neV), ^{58}Ni (∼350 neV). Relevant for EDM experiments are also non-metallic insulator materials, e.g., SiO_2 (∼90 neV) or Al_2O_3 (∼150 neV).

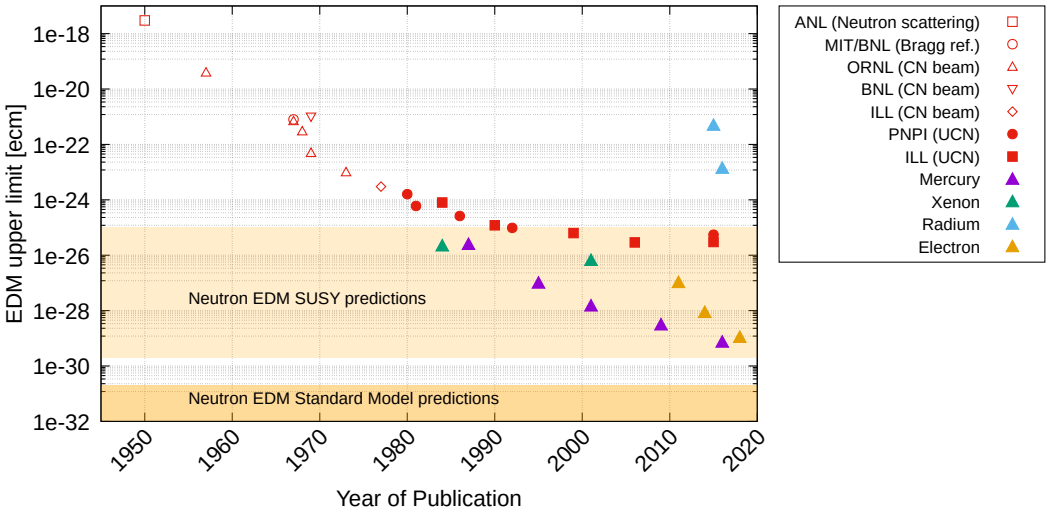

Figure 2. Experimental progress of EDM searches showing published upper limits for the neutron, the electron and atoms. Tremendous improvements on sensitivities have been achieved from early neutron beam to modern ultra cold neutron storage experiments. The superior EDM measurement with the highest sensitivity was conducted using the diamagnetic atom ^{199}Hg. Recent remarkable results come from electron EDM searches, using highly polarizable molecules. An example of a new candidate is the ^{225}Ra EDM experiment using trapped atoms with heavy nuclei.

The last improvement of sensitivity on the EDM of the neutron with the result of $d_{\mathrm{n}} < 2.9 \times 10^{-26}$ $e$cm (90% C.L.) by the ILL/RAL/Sussex collaboration [7] was enabled by introducing a mercury (^{199}Hg) comagnetometer. The apparatus used is described in detail in [20]. Polarized UCN were filled into a storage cell located inside a four-layer magnetic shield. Ramsey's method of separated oscillatory fields was employed to determine the phase accumulated by the neutrons during a free precession period of applied magnetic and electric fields. UCNs are counted after measurements at four different working points using off-resonant spin-flip frequencies. Their precession frequency is determined by fitting the data to the Ramsey fringe curve.

The statistical sensitivity to an EDM σ_{d} is determined by

$$\sigma_{\mathrm{d}} = \frac{\hbar}{2\alpha E T\sqrt{N}}, \tag{3}$$

where α is the visibility (depending on initial spin polarization, spin lifetime and analyzer efficiency), E the electric field strength, T the free spin precession time and N the number of neutrons. Next generation experiments mainly rely on a significant improvement on N limited mainly by the yield of current UCN sources, but also by efficient UCN transport. Another major focus to achieve better EDM sensitivity is improvement on leading systematic effects, which are currently dominated by magnetic field quality.

A challenging new approach to overcome limitations by measuring the neutron EDM in situ, i.e., inside the UCN production volume filled with superfluid helium, is being pursued at the ORNL spallation neutron source. In addition, new efforts reviving neutron EDM searches using crystal diffraction [21] and a neutron beam [22] are proposed. Most next generation neutron EDM experiments (ILL, PSI, FRM-II and TRIUMF) are based on previously employed concepts of a room-temperature UCN storage cell with internal comagnetometery surrounded by various magnetometers. However, experiments are using different types of UCN sources, the "UCN turbine" (PNPI-ILL), solid deuterium UCN sources (PSI, FRM-II, LANL) and superfluid helium UCN sources (ILL PanEDM, TRIUMF, ORNL).

4. Neutron EDM Project and UCN Facility at TRIUMF

The planned neutron EDM experiment at TRIUMF is based on a room-temperature storage cell located inside a large multi-layer magnetic shield and filled with UCNs produced in a superfluid helium source. The electric field of up to 13 kV/cm is applied to an electrode centered in a stack of two storage cells with ground electrodes on their outer faces. The double cell combined with simultanous neutron spin detection allows for measurements of neutron spin precession frequencies for both alignments of magnetic and electric field in a single fill cycle. For an improved understanding of systematic effects related to magnetic field quality, both an array of spin-exchange relaxation free (SERF) magnetometers [23] and a second comagnetometer species are anticipated to be implemented in the experiment. The additional comagnetometer species ^{129}Xe, with a magnetic moment of same sign as the neutron magnetic moment, provides a second measurement of the magnetic field, complementing the ^{199}Hg comagnetometer. The dual species comagnetometer enables the determination of vertical magnetic field as well as the vertical magnetic field gradient to correct for a false neutron EDM signal arising from the geometric phase effect [19,24].

To meet the statistics requirements for an anticipated sensitivity of 10^{-27} $e$cm, the TUCAN (TRIUMF Ultra Cold Advanced Neutron source) collaboration is developing a strong, world-leading UCN source to generate a UCN density of several hundreds of UCN per cm^3 in the EDM storage cells. A secondary goal is to establish a leading UCN user facility at TRIUMF. The first milestone towards the new UCN facility has been reached in 2016 with commissioning of the UCN beamline.

4.1. UCN Beamline

The UCN beamline at TRIUMF is designed to allow sharing of proton beams between other users and UCN. A kicker magnet operated by a power supply ramping to full current of 180 A within 50 µs enables diverting 520 MeV proton bunches from TRIUMF beamline 1A onto the UCN spallation target. An average current of up to 40 µA can be taken from the maximum current of 120 µA in beamline 1A allowing simultaneous operation with other users at TRIUMF. Details on the beamline can be found in a recently submitted publication [25].

4.2. UCN Source and First Production Results

In early 2017, a prototype UCN source developed and formerly operated at RCNP [26] was installed at TRIUMF. The thermal neutrons created in the UCN spallation target are slowed down in two moderator stages of D_2O at room temperature and ice D_2O at 20 K before being converted to UCN in a He-II volume. Slow neutrons ($E_{\mathrm{kin}} \sim$ meV) can be efficiently scattered in liquid helium and lose almost all of their kinetic energy to phonon excitations [27,28]. A critical parameter for the UCN production yield is the temperature of the He-II, as unfavorable upscattering processes scale with temperature as $\sim T^7$, but can be strongly suppressed by cooling the He-II to temperatures of $\sim$1 K and below.

The protoype UCN source uses 8 L of He-II as UCN production volume reaching a minimum temperature of 0.85 K when idling at static heat load of $\approx$0.1 W. Due to the additional heat load during target irradiation, the He-II temperature during production increases and the maximum UCN source lifetime measured at RCNP was 81 s, significantly below the expected $\sim$400 s at 0.85 K. He-II inside the UCN production volume is cooled via a He-II filled channel to a heat-exchanger thermally connected to a liquid ^{3}He bath. The ^{3}He bath is cooled to 0.73 K by lowering the vapour pressure to $<$2 Torr via pumping. Pre-cooling of the circulated ^{3}He gas is accomplished through two cooling stages using natural helium at 4 K and at 1.6 K, the latter cooled by lowering the vapor vapour pressure through pumping.

Using the prototype UCN source, the first UCNs at TRIUMF were successfully produced in November 2017. In the initial measurements, we obtained yields of 40,000 and 300,000 detected UCNs at a proton beam current of 1 µA and 10 µA, respectively, when irradiating the spallation target for 60 s.

The linear scaling of UCN yield with proton current was demonstrated at shorter irradiation times of 30 s, which was necessary to reduce effects from beam heating. More details and further results can be found in a recently submitted paper [29].

With successful demonstration of UCN production using the prototype source, the facility is now available for tests of components for the new UCN source and equipment for the neutron EDM experiment.

4.3. Design of a New UCN Source at TRIUMF

The new UCN source under development for the TRIUMF UCN user facility and the neutron EDM experiment will use an improved, more efficient cooling concept also based on a heat-exchanger connected to a ^{3}He bath. Additionally, improvements are anticipated from using a combination of heavy water and liquid deuterium (LD_2) as moderators.

The design was highly optimized by simulations in terms of geometry and volume of LD_2 and He-II with a maximum allowable heat load on the He-II of 10 W at 1.15 K. In the resulting layout with a long horizontal He-II section of 70 L volume (of which 34 L are the UCN production volume), the main considerations for cryogenics are thermal conductivity through He-II and the heat-exchanger. Both are limiting the heat transfer from the UCN production volume close to the spallation target to the ^{3}He bath side of the heat-exchanger. Transfer through He-II is accounted for by appropriate sizing of the He-II volume in terms of diameter and length, while thermal conductivity of the heat-exchanger is mainly limited by the Kapitza resistance of the nickel-plated copper to He-II boundary surface. Test measurements of the Kapitza conductance done at KEK showed very promising results eliminating a major cryogenic design risk.

Figure 3 shows a draft design of the new UCN source layout and geometry. The temperature goal of the UCN production volume of 1.15 K allows for sufficiently long storage lifetimes in He-II while locating the source cryostat far away in an area with reduced radiation levels. The 34 L UCN production volume of superfluid, isotopically purified ^{4}He are kept at an operating temperature of 1.15 K during a period of 60 s of target irradiation with a proton beam power of 20 kW (40 μA of 520 MeV protons). The full proton beam power produces a heat load on the order of 10 W to the He-II inside the UCN production volume close to the target. The cooling power required to keep the ^{3}He side of the heat-exchanger at ∼0.8 K is provided by a pumping system capable of sustaining a ^{3}He throughput of 1.12 g/s (or 10,300 m^3/h). The peak design mass flow is based on assuming a full transfer of the 10 W heat load through the heat-exchanger to the ^{3}He bath.

From simulations and the optimization process, the new UCN source is expected to produce about 10^7 UCN/s. This improvement of two orders of magnitude compared to the prototype UCN source is driven mainly by enabling operation at full proton beam current of 40 μA, a four-fold increased He-II production volume close to the spallation target and an improved moderator concept using LD_2 rather than ice D_2O.

The new UCN source at TRIUMF is scheduled to be installed during the main shutdown in early 2021 with first UCN production expected by the end of 2021. Successful commissioning of the new UCN source facilitates the neutron EDM experiment at TRIUMF anticipated to start taking data in 2022 with the goal of achieving a sensitivity to an EDM of the neutron on the order of 10^{-27} *e*cm within less than 500 measurement days.

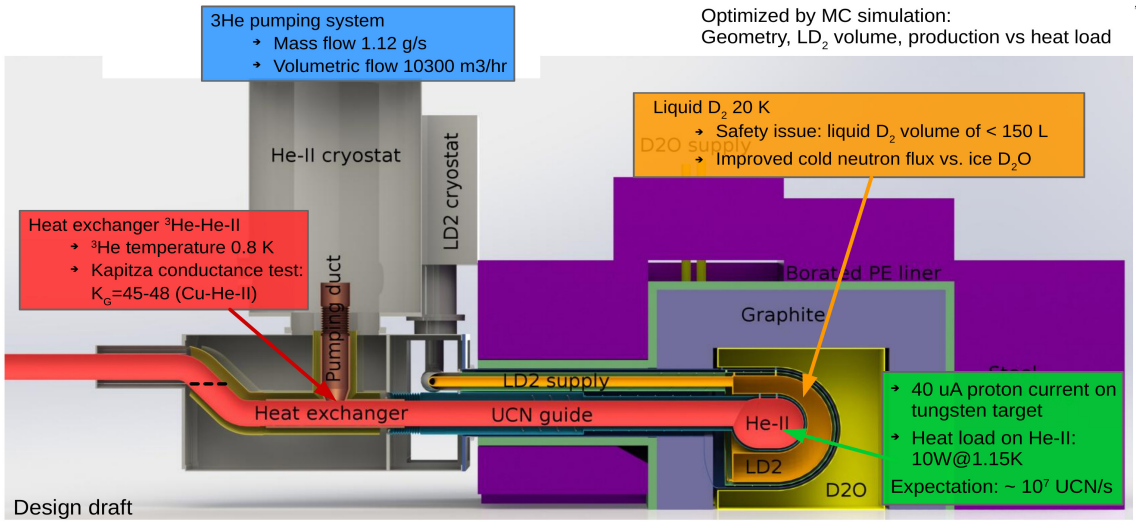

Figure 3. Draft design of the new ultra cold neutron (UCN) source at TRIUMF. The superfluid helium (He-II) UCN production volume is kept below 1.15 K during target irradiation causing a heat load of about 10 W. Cooling of He-II inside the 34 L production volume and a long UCN guide is provided through a heat-exchanger with a UCN friendly side of nickel plated copper thermally connected to the ^{3}He bath at 0.8 K. The ^{3}He fridge is designed to provide 10 W of cooling power resulting in a required pumping speed of 1.12 g/s. With heavy water (D_2O) and liquid deuterium (LD_2) moderator vessels and a full UCN beam current of 40 μA, the UCN source is expected to produce $\sim 10^7$ UCN/s.

5. Xenon EDM Experimental Status

Results from searches for atomic EDMs as more complex systems than the neutron make additional manifestations of new physics accessible due to the electron EDM or *CP*-odd interactions between nuclei and between nuclei and electrons. While paramagnetic atoms or molecules are particularly sensitive to an electron EDM with only higher order contributions involving nuclei, diamagnetic atoms such as ^{199}Hg, ^{129}Xe or ^{225}Ra exhibit many *CP*-odd processes contributing to an EDM (c.f. Figure 1).

The current limit on an EDM of ^{129}Xe was published in 2001 [11], with the result of $d_{\mathrm{Xe}} < 6.6 \times 10^{-27}$ *e*cm (95% C.L.). The experiment was based on a spin maser driving nuclear spin polarizations of the two noble gas species ^{3}He and ^{129}Xe, where ^{3}He was used as a comagnetometer. With continuously supplying polarized gas diffusing from a pump cell attached to the EDM cell with high voltage electrodes, the maser technique can achieve almost continuous long-term observation. The main limitation in the experiment was the stability of the feedback electronics.

There are currently three ongoing efforts towards a new limit of the EDM of ^{129}Xe; an improved version of the spin maser using an optical readout of the nuclear spin precession [30] and two similar approaches followed by the MIXed [31] and HeXeEDM collaborations [32] using a sample of freely precessing ^{3}He and ^{129}Xe nuclear spins detected by SQUID sensors.

6. Progress towards a New Measurement of the EDM of ^{129}Xe: HeXeEDM

The HeXeEDM collaboration is seeking to improve the upper limit on an EDM of the diamagentic isotope ^{129}Xe by one to two orders of magnitude compared to the current limit of 6.6×10^{-27} *e*cm [11]. The HeXeEDM experiment also uses a ^{3}He comagnetometer, but with freely precessing nuclear spins of ^{3}He and ^{129}Xe in a highly shielded magnetically stable environment rather than a driven oscillation as in the nuclear spin maser. Very long observation times in excess of several hours are accessible inside a large magnetically shielded room (MSR) with particularly low residual magnetic field gradients. Because of the high magnetic field quality, long spin relaxation time constants are possible even at high pressure of the noble gas species inside the EDM cell, as no motional narrowing is required to average field inhomogeneities. In turn, the high total gas pressure of 0.5 to 1.0 bar allows high electric

field strengths without the need of buffer gases. New EDM cells have been developed using glass cylinders (Pyrex) with heat bonded silicon electrodes and a glass valve attached to one electrode with a center hole. Nuclear spin precession of the two noble gas species is detected by highly sensitive SQUID sensors with magnetic field noise below 10 fT/$\sqrt{\text{Hz}}$, allowing for large signal-to-noise ratios.

A high nuclear spin polarization—orders of magnitude above the thermal polarization—is generated in a spin-exchange optical pumping (SEOP) setup where both noble gas species are simultaneously polarized via spin-exchange collisions with optically pumped rubidium vapour [33]. The optical pumping cell is placed inside an oven to increase the vapour density of rubidium, particularly for efficient spin exchange to ^{3}He. Typically, ^{3}He is first polarized for several hours at temperatures of >140 °C, before the temperature is lowered for several minutes to efficiently polarize ^{129}Xe at ∼80 °C. The gas mixture of polarized ^{3}He and ^{129}Xe as well as nitrogen quenching gas—typically in ratios of ^{3}He:^{129}Xe:N_2 = 75:15:10—is filled into an evacuated EDM cell in the fringe field of the polarizer magnetic holding field (∼3 mT). The EDM cell is then transported into a MSR avoiding zero magnetic field crossings and placed underneath a liquid helium dewar with six SQUID sensors. A grounding silicon wafer protects the sensitive SQUIDs from damage due to possible discharges (c.f. Figure 4). After applying a transverse $\pi/2$ spin flip pulse combined for both species, the nuclear spin precession in the magnetic holding field (1–2 µT) is recorded, while a sequence of zero, $+E$ and $-E$ electric field ($E \approx 3$ kV/cm) is applied.

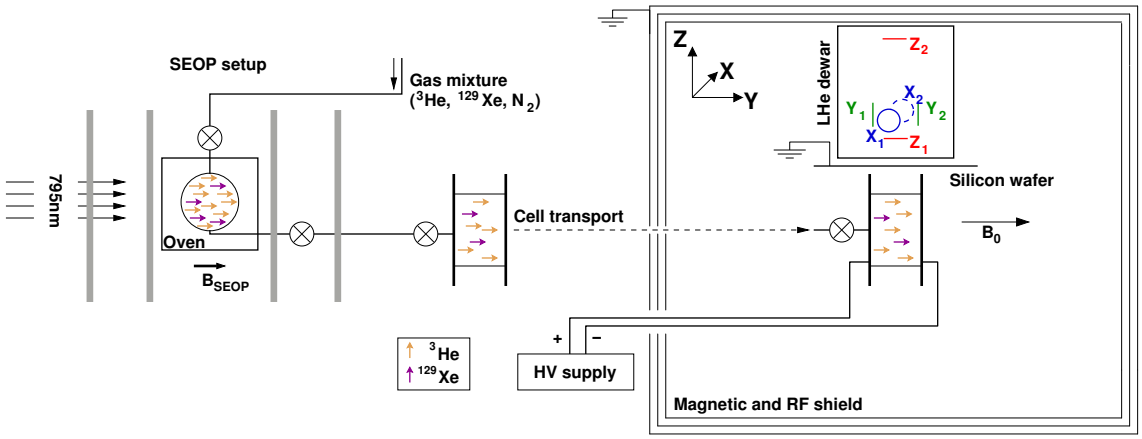

Figure 4. Scheme of the HeXeEDM experimental setup: In a spin-exchange optical pumping (SEOP) setup located outside a magnetically shielded room (MSR), the noble gas nuclei of ^{3}He and ^{129}Xe are simultaneously spin polarized. After filling the polarized gas mixture into an evacuated EDM cell, the cell is transported into the MSR and placed underneath a liquid helium dewar housing SQUID sensors. After an initial spin flip, nuclear spin precession of both species is detected in applied magnetic (∼1–2 µT) and electric (∼3 kV/cm) fields.

Initial test measurements and developments were done in the MSR at FRM-II [34], with further details on the experimental setup available in [32]. A main systematic effect, i.e., drift of the comagnetometer corrected frequencies, was investigated with important implications on the comagnetometer approach and understanding of the observed drifts [35]. The MSR at FRM-II moved to ILL (Grenoble) in 2017 to be used as a magnetic shield for a neutron EDM measurement. The HeXeEDM experiment relocated to PTB Berlin, where several weeks of tests and EDM measurement runs were taken out in 2017 and 2018 inside the BMSR-2 [36]. In both runs, many systematic effects were investigated and several parameters varied during EDM measurements, i.e., high-voltage ramp speed, high-voltage dwell times, high-voltage starting polarity, EDM cells, magnetic holding field direction and total gas pressure.

Data of 120 individual EDM measurements were recorded within one week in 2017 and are currently in the final stage of data analysis. Sources and sizes of systematic effects are being evaluated and the final result is expected to be comparable to the most recent published limit [11].

The EDM run in 2018 is not yet included in the analysis, but typically had a ten-fold larger ^{3}He comagnetometer signal due to better polarizations achieved in the SEOP setup.

For the next EDM run, a liquid helium dewar with lower intrinsic noise and a better understanding will be used and hence reduction of major systematic effects is anticipated. An improvement in sensitivity by at least one order of magnitude is expected.

7. Conclusions

Searches for permanent EDMs of fundamental particles and atoms provide a direct probe of time-reversal violation and physics beyond the SM. Results from EDM experiments have put strong constraints on many new physics models, which typically require larger EDMs. In a global analysis, the combination of many EDM results using different systems can improve limits on *CP* violating sources compared to a sole-source analysis. Hence, even with the superior sensitivity of the ^{199}Hg EDM measurement, further effort is necessary on other systems for a more detailed understanding of the underlying physics.

Of the many neutron EDM experiments around the world, the first are expected to start taking data within the next years with the goal to improve the sensitivity by at least an order of magnitude. Progress is to be expected soon on the EDM sensitivity of diamagnetic atoms, e.g., ^{129}Xe and from new experiments using heavy isotopes, like ^{225}Ra. New measurements will provide a better insight into *CP* violating fundamental processes and the implications for physics beyond the SM.

Funding: Research within the TUCAN collaboration was funded by the Canadian Foundation for Innovation (CFI), the Canada Research Chairs program, the Japan Society for the Promotion of Science (JSPS) the Natural Sciences and Engineering Research Council of Canada (NSERC), and Research Manitoba. Research within the HeXeEDM collaboration was supported in part by NSF grant PHY-1506021, DOE grant DE-FG0204ER41331, Michigan State University, by Deutsche Forschungsgemeinschaft grants TR408/12 and FA1456/1-1 and the Cluster of Excellence "Origin and Structure of the Universe".

Acknowledgments: For the TUCAN collaboration I would like to thank C. Marshall, T. Hessels, S. Horn and D. Rompen for engineering support, B. Hitti and C. Dick for supplying liquid helium, G. Remon and D. Morris for support with controls, and TRIUMF Operations Group for delivering beam. For the HeXeEDM collaboration I would like to thank P. Pistel and R. Wentz for innovation in glass blowing and cell construction.

Conflicts of Interest: The author declares no conflict of interest.

References

1. Collaboration P.; Ade, P.A.R.; Aghanim, N.; Armitage-Caplan, C.; Arnaud, M.; Ashdown, M.; Atrio-Barandela, F.; Aumont, J.; Baccigalupi, C.; Banday, A.J.; et al. Planck 2013 results. XVI. Cosmological parameters. *Astron. Astrophys.* **2014**, *571*, A16. [CrossRef]
2. Iocco, F.; Mangano, G.; Miele, G.; Pisanti, O.; Serpico, P.D. Primordial nucleosynthesis: From precision cosmology to fundamental physics. *Phys. Rep.* **2009**, *472*, 1–76. [CrossRef]
3. Sakharov, A.D. Violation of CP Invariance, C Asymmetry, and Baryon Asymmetry of the Universe. *Pisma Zh. Eksp. Teor. Fiz.* **1967**, *5*, 32–35. [CrossRef]
4. Trodden, M. Electroweak baryogenesis. *Rev. Mod. Phys.* **1999**, *71*, 1463–1500. [CrossRef]
5. Schiff, L.I. Measurability of Nuclear Electric Dipole Moments. *Phys. Rev.* **1963**, *132*, 2194–2200. PhysRev.132.2194. [CrossRef]
6. Pospelov, M.; Ritz, A. Electric dipole moments as probes of new physics. *Ann. Phys.* **2005**, *318*, 119–169. doi:10.1016/j.aop.2005.04.002. [CrossRef]
7. Baker, C.A.; Doyle, D.D.; Geltenbort, P.; Green, K.; van der Grinten, M.G.D.; Harris, P.G.; Iaydjiev, P.; Ivanov, S.N.; May, D.J.R.; Pendlebury, J.M.; et al. Improved Experimental Limit on the Electric Dipole Moment of the Neutron. *Phys. Rev. Lett.* **2006**, *97*, 131801; doi:10.1103/PhysRevLett.97.131801. [CrossRef]
8. Peccei, R.D.; Quinn, H.R. CP Conservation in the Presence of Pseudoparticles. *Phys. Rev. Lett.* **1977**, *38*, 1440–1443. [CrossRef]
9. Khriplovich, I.B.; Zhitnitsky, A.R. What is the value of the neutron electric dipole moment in the Kobayashi-Maskawa model? *Phys. Lett. B* **1982**, *109*, 490–492. [CrossRef]

10. Graner, B.; Chen, Y.; Lindahl, E.G.; Heckel, B.R. Reduced Limit on the Permanent Electric Dipole Moment of 199Hg. *Phys. Rev. Lett.* **2016**, *116*, 161601. [CrossRef]
11. Rosenberry, M.A.; Chupp, T.E. Atomic Electric Dipole Moment Measurement Using Spin Exchange Pumped Masers of ^{129}Xe and ^{3}He. *Phys. Rev. Lett.* **2001**, *86*, 22–25. [CrossRef] [PubMed]
12. Bishof, M.; Parker, R.H.; Bailey, K.G.; Greene, J.P.; Holt, R.J.; Kalita, M.R.; Korsch, W.; Lemke, N.D.; Lu, Z.T.; Mueller, P.; et al. Improved limit on the 225Ra electric dipole moment. *Phys. Rev. C* **2016**, *94*, 025501. [CrossRef]
13. Collaboration, A.; Andreev, V.; Ang, D.G.; DeMille, D.; Doyle, J.M.; Gabrielse, G.; Haefner, J.; Hutzler, N.R.; Lasner, Z.; Meisenhelder, C.; et al. Improved limit on the electric dipole moment of the electron. *Nature* **2018**, *562*, 355. [CrossRef] [PubMed]
14. Ellis, J. Theory of the neutron electric dipole moment. *Nucl. Instrum. Methods Phys. Res. Sect. A* **1989**, *284*, 33–39. [CrossRef]
15. Donoghue, J.F.; Holstein, B.R.; Musolf, M.J. Electric dipole moments of nuclei. *Phys. Lett. B* **1987**, *196*, 196–202. [CrossRef]
16. Sushkov, O.P.; Flambaum, V.V.; Khriplovich, I.B. Possibility of investigating P- and T-odd nuclear forces in atomic and molecular experiments. *Sov. Phys. JETP* **1984**, *60*, 873.
17. Ng, D.; Ng, J.N. A note on Majorana neutrinos, leptonic CKM and electron electric dipole moment. *Mod. Phys. Lett. A* **1996**, *11*, 211–216. [CrossRef]
18. Chupp, T.; Ramsey-Musolf, M. Electric dipole moments: A global analysis. *Phys. Rev. C* **2015**, *91*, 035502. [CrossRef]
19. Masuda, Y.; Asahi, K.; Hatanaka, K.; Jeong, S.C.; Kawasaki, S.; Matsumiya, R.; Matsuta, K.; Mihara, M.; Watanabe, Y. Neutron electric dipole moment measurement with a buffer gas comagnetometer. *Phys. Lett. A* **2012**, *376*, 1347–1351. [CrossRef]
20. Baker, C.A.; Chibane, Y.; Chouder, M.; Geltenbort, P.; Green, K.; Harris, P.G.; Heckel, B.R.; Iaydjiev, P.; Ivanov, S.N.; Kilvington, I.; et al. Apparatus for measurement of the electric dipole moment of the neutron using a cohabiting atomic-mercury magnetometer. *Nucl. Instrum. Methods Phys. Res. Sect. A* **2014**, *736*, 184–203. [CrossRef]
21. Fedorov, V.V.; Jentschel, M.; Kuznetsov, I.A.; Lapin, E.G.; Lelièvre-Berna, E.; Nesvizhevsky, V.; Petoukhov, A.; Semenikhin, S.Y.; Soldner, T.; Voronin, V.V.; et al. Measurement of the neutron electric dipole moment via spin rotation in a non-centrosymmetric crystal. *Phys. Lett. B* **2010**, *694*, 22–25. [CrossRef]
22. Piegsa, F.M. New concept for a neutron electric dipole moment search using a pulsed beam. *Phys. Rev. C* **2013**, *88*, 045502. [CrossRef]
23. Allred, J.C.; Lyman, R.N.; Kornack, T.W.; Romalis, M.V. High-Sensitivity Atomic Magnetometer Unaffected by Spin-Exchange Relaxation. *Phys. Rev. Lett.* **2002**, *89*, 130801. [CrossRef] [PubMed]
24. Pendlebury, J.M.; Heil, W.; Sobolev, Y.; Harris, P.G.; Richardson, J.D.; Baskin, R.J.; Doyle, D.D.; Geltenbort, P.; Green, K.; van der Grinten, M.G.D.; et al. Geometric-phase-induced false electric dipole moment signals for particles in traps. *Phys. Rev. A* **2004**, *70*, 032102. [CrossRef]
25. Ahmed, S.; Andalib, T.; Barnes, M.J.; Bidinosti, C.B.; Bylinsky, Y.; Chak, J.; Das, M.; Davis, C.A.; Franke, B.; Gericke, M.T.W.; et al. A Beamline for Fundamental Neutron Physics at TRIUMF. *arXiv* **2018**, arXiv:1810.01001.
26. Masuda, Y.; Hatanaka, K.; Jeong, S.C.; Kawasaki, S.; Matsumiya, R.; Matsuta, K.; Mihara, M.; Watanabe, Y. Spallation Ultracold Neutron Source of Superfluid Helium below 1 K. *Phys. Rev. Lett.* **2012**, *108*, 134801. [CrossRef] [PubMed]
27. Golub, R.; Pendlebury, J.M. Super-thermal sources of ultra-cold neutrons. *Phys. Lett. A* **1975**, *53*, 133–135. [CrossRef]
28. Golub, R.; Pendlebury, J.M. The interaction of Ultra-Cold Neutrons (UCN) with liquid helium and a superthermal UCN source. *Phys. Lett. A* **1977**, *62*, 337–339. [CrossRef]
29. Ahmed, S.; Altiere, E.; Andalib, T.; Bell, B.; Bidinosti, C.; Cudmore, E.; Das, M.; Davis, C.; Franke, B.; Gericke, M.; et al. First ultracold neutrons produced at TRIUMF. *arXiv* **2018**, arXiv:1809.04071.
30. Sato, T.; Ichikawa, Y.; Ohtomo, Y.; Sakamoto, Y.; Kojima, S.; Funayama, C.; Suzuki, T.; Chikamori, M.; Hikota, E.; Tsuchiya, M.; et al. EDM measurement in ^{129}Xe atom using dual active feedback nuclear spin maser. *Hyperfine Interact.* **2015**, *230*, 147–153. [CrossRef]

31. Heil, W.; Gemmel, C.; Karpuk, S.; Sobolev, Y.; Tullney, K.; Allmendinger, F.; Schmidt, U.; Burghoff, M.; Kilian, W.; Knappe-Grüneberg, S.; et al. Spin clocks: Probing fundamental symmetries in nature. *Ann. Phys.* **2013**, *525*, 539–549. [CrossRef]
32. Kuchler, F.; Babcock, E.; Burghoff, M.; Chupp, T.; Degenkolb, S.; Fan, I.; Fierlinger, P.; Gong, F.; Kraegeloh, E.; Kilian, W.; et al. A new search for the atomic EDM of 129Xe at FRM-II. *Hyperfine Interact.* **2016**, *237*, 95. [CrossRef]
33. Walker, T.G.; Happer, W. Spin-exchange optical pumping of noble-gas nuclei. *Rev. Mod. Phys.* **1997**, *69*, 629–642. [CrossRef]
34. Altarev, I.; Babcock, E.; Beck, D.; Burghoff, M.; Chesnevskaya, S.; Chupp, T.; Degenkolb, S.; Fan, I.; Fierlinger, P.; Frei, A.; et al. A magnetically shielded room with ultra low residual field and gradient. *Rev. Sci. Instrum.* **2014**, *85*, 075106. [CrossRef] [PubMed]
35. Terrano, W.A.; Meinel, J.; Sachdeva, N.; Chupp, T.; Degenkolb, S.; Fierlinger, P.; Kuchler, F.; Singh, J.T. Frequency shifts in Noble-Gas Magnetometers. *arXiv* **2018**, arXiv:1807.11119.
36. Bork, J.; Hahlbohm, H.D.; Klein, R.; Schnabel, A. The 8-layered magnetically shielded room of the PTB: Design and construction. In Proceedings of the 12th International Conference on Biomagnetism, Espoo, Finland, 13–17 August 2000.